Effects of Reactant Concentrations on Reactive Miscible Viscous Fingering

Yuichiro Nagatsu and Toshihisa Ueda
School of Science for Open and Environmental Systems, Keio University, Yokohama, Kanagawa, 223-8522, Japan

Effects of reactant concentrations on the characteristics of reactive miscible viscous fingering in a Hele-Shaw cell at low finger-growth velocity were studied both experimentally and theoretically. The product distribution varies with the variations in the initial reactant concentrations and depends on the location of a reaction zone. When the reaction zone is located in the more-viscous-liquid region the product concentrates at the fingertips, but when it is located in the less-viscous-liquid region, the product spreads in a relatively broad area inside the fingers. This significant difference in the reaction pattern resulting from variations in the reactant concentrations is caused by the large difference of molecular diffusivity in the two liquids, that is, of viscosity which is one of the important factors for viscous fingering. These results are confirmed theoretically by one-dimensional diffusive–reactive analysis.

Introduction

Viscous fingering in flows is a ubiquitous instability occurring when a fluid with low mobility is displaced by another fluid with high mobility. The difference in mobility can originate from a difference between the two fluids in viscosity and/or density. Fingering instability takes place in both miscible and immiscible cases. Surface tension in immiscible systems plays an important role in the fingering mechanism, while in the miscible systems convective and diffusive effects are important (Homsy, 1987).

Of particular interest in the present study is the miscible viscous fingering in two reactive fluids in which a chemical reaction takes place. There are many applications for reactive miscible viscous fingering in which an interaction between chemistry and hydrodynamics takes place. These applications include petroleum recovery (Homsy, 1987), the spreading of reactive pollutants in groundwater, fixed-bed chemical processing and regeneration (Homsy, 1987), frontal polymerization (Pojman et al., 1998), chromatographic and adsorptive separations (Dickson et al., 1997; Shalliker et al., 1999), reactive infiltration in geochemical settings (DeWit and Homsy, 1999a), deformation of chemical waves by hydrodynamical instabilities (Carey et al., 1996; Vasquez, 1997; Eckert and Grahn, 1999), and even medical applications related to blood-clot dissolution in coronary thrombi (Zidansek et al., 1995) and gastric mucus (Bhaskar et al., 1992; Chu et al., 1999).

From the viewpoint of enhancing the mixing and chemical reactions of fluids, it is desirable to induce flow turbulence if the fluids are gases or less-viscous liquids. It is, however, difficult to induce flow turbulence when the fluids are more-viscous liquids. In such cases, a viscous fingering system is thought to be effective in enhancing the mixing and chemical reactions, because fingering produces a larger contact surface area between two liquids.

In spite of these broad applications, there is still little fundamental understanding of the nature of the coupling between chemistry and hydrodynamics in reactive miscible viscous fingering. Although DeWit and Homsy have recently investigated numerically reactive miscible viscous fingering in porous media (DeWit and Homsy, 1999a,b), it is generally quite difficult to find experimental studies on this issue.

Regarding the fluid dynamics of viscous fingering without chemical reaction, numerous numerical and experimental studies of both miscible and immiscible systems have been reported in the last 50 years (Homsy, 1987; Tanveer, 2000). The flows in a Hele-Shaw cell consisting of two closely plane-parallel plates have been used to model the flows in porous media and have often been used to study viscous fingering (Homsy, 1987). Viscous fingering instability can be experimentally observed when a less-viscous fluid displaces a

Correspondence concerning this article should be addressed to T. Ueda.

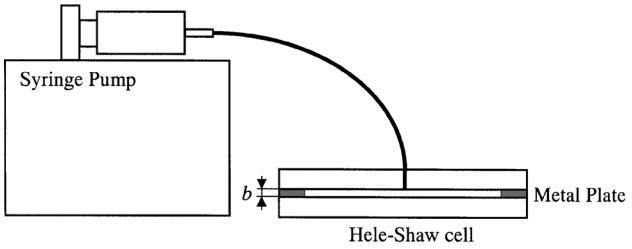

Figure 1. Experimental apparatus.

more-viscous one in a Hele-Shaw cell, and many important results have been reported.

With regard to the study of viscous fingering with chemical reaction in a Hele-Shaw cell, only a few investigations focusing on medical applications (Bhaskar et al., 1992) and on oil recovery (Hornof and Baig, 1995) have been reported. However, few investigations from the fundamental viewpoint of the relationship between chemistry and hydrodynamics have been carried out. The objective of the present study is therefore to investigate experimentally the characteristics of reactive miscible viscous fingering using a Hele-Shaw cell, and to discuss the relationship between chemistry and hydrodynamics. We especially focus on the effects of variations in the reactant concentrations in two liquids on the characteristics of the chemical reaction in miscible viscous fingering. The phenomena observed experimentally are discussed from a theoretical viewpoint to elucidate the diffusion–chemical-reaction mechanism in viscous fingering.

Experimental Apparatus and Procedure

Figure 1 shows an experimental apparatus, a syringe pump that injects liquids at a constant volumetric flow rate with high accuracy, and a Hele-Shaw cell consisting of two closely spaced plane-parallel plates. The Hele-Shaw cell is formed by two 140 mm × 140 mm × 10 mm transparent glass plates spaced with a constant gapwidth b. The gapwidth b is set as $b = 0.24$ mm by placing four metal triangular plates at four corners between two glass plates. The upper glass plate has a small hole drilled in the center for liquid injection. The constant gapwidth throughout the cell was confirmed by the method of Chen (1989). The more-viscous liquid initially occupies the cell. The less-viscous one that reacts with the more-viscous one is injected at a constant volumetric flow rate $q = 0.94$ mm^3/s by the syringe pump from the small hole in the upper glass plate. Experiments are conducted by varying the initial molar concentration of reactant in the more-viscous liquid (c_{m0}) and that in the less-viscous liquid (c_{l0}) to elucidate the effects of reactant concentrations on the characteristics of reactive miscible viscous fingering. An experiment with nonreactive liquids is also conducted in order to compare the reactive and nonreactive cases. The motion of the miscible viscous fingering and the chemical reaction in the cell are recorded with a digital video camera placed below the cell for further analysis.

In the reactive cases, a mixture of 99 wt % glycerin and 1 wt % KSCN solution is used as the more-viscous liquid, and a $Fe(NO_3)_3$ solution as the less-viscous one. A product that is blood red in color is generated by the chemical reaction as follows

$$Fe^{3+}\ (\text{light yellow}) + 2SCN^{-}\ (\text{colorless}) \rightarrow [Fe(SCN)_2]^{+}\ (\text{blood red}). \quad (1)$$

In this reaction, the blood-red product is easily recognizable. The heat release due to the chemical reaction is negligible, meaning that the chemical reaction is passive for the flow motion. In the nonreactive case, a colorless mixture of 99 wt. % glycerin and 1 wt % water is used as the more-viscous liquid, and the blood-red $[Fe(SCN)_2]^+$ solution formed by Reaction 1 between a 0.05 mol/L $Fe(NO_3)_3$ solution and a 0.1 mol/L KSCN solution is used as the less-viscous one. In all experiments, the viscosity of the more-viscous liquid, μ_m, is 1.2 Pa·s, and that of the less-viscous liquid, μ_l, is 1.0×10^{-3} Pa·s. All experiments were run at room temperature, 20°C.

The Peclet number, Pe_v, which is the ratio of the transport rate by convection and that by diffusion, is defined the same as that by Petitjeans et al. (Petitjeans et al., 1999), as follows

$$Pe_v = \frac{LU}{D_v} = \frac{R\dfrac{q}{2\pi Rb}}{D_v} = \frac{q}{2\pi bD_v} \quad (2)$$

Here, the characteristic length L is equal to radius R, and the characteristic velocity U is equal to $q/2\pi Rb$. The averaged molecular diffusion coefficient between water and glycerin, which is 1.6×10^{-4} mm^2/s (Petitjeans and Maxworthy, 1996), is D_v. In all experiments, Pe_v is set as $Pe_v = 3.9 \times 10^3$.

The most distinctive feature of reactive miscible viscous fingering is that products are formed, that is, the system consists of more than three components; in contrast, the nonreactive system consists of only two components, the less- and more-viscous liquids. In other words, the existence of products is the distinguishing feature of chemically reactive flows. In addition, when we deal with chemically reactive flows, it is generally important to consider whether a chemical reaction is active or passive for a flow field. Since the reaction is passive for a flow field in the present study, the reaction characteristics are examined by comparing the reactive and nonreactive cases, because hydrodynamic characteristics in those cases are supposed to be very similar. Therefore, we examined the characteristics of a chemical reaction in a viscous fingering system, paying close attention to the product region and quantity, and comparing reactive and nonreactive cases.

Results and Discussion

Experiment

Figure 2 shows the miscible viscous fingering pattern without chemical reaction at $t = 390$ s. A well-defined interface between two miscible liquids is formed, as the Peclet number is $Pe_v = 3.9 \times 10^3$ (Petitjeans and Maxworthy, 1996; Rakotomalala et al, 1997). The depth of the blood-red color is light at the fingertips, indicating that the less-viscous-liquid layer becomes thin there, which is similar to "an internal shock" observed in miscible displacement (Lajeunesse et al., 1999).

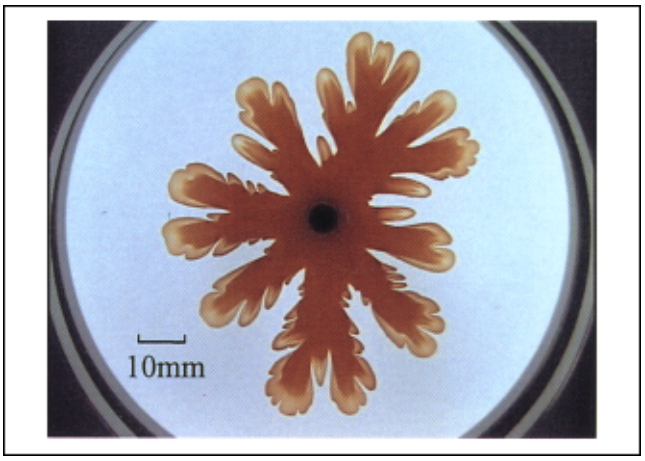

Figure 2. Miscible viscous fingering pattern without chemical reaction at $t = 390$ s.

Figure 3 shows the temporal evolution of miscible viscous fingering with the chemical reaction under conditions with $c_{m0} = 0.08$ mol/L and $c_{l0} = 0.04$ mol/L, which is the stoichiometric ratio of Eq. 1. In this figure, the product region is the blood-red region, and the depth of the color corresponds to the product quantity. At $t = 30$ s, small fingers can be observed, and the entire region of the less-viscous liquid is blood red. This result indicates that the chemical reaction starts immediately after injection, indicating that the chemical reaction is much faster than the fluid dynamical motion. In other words, the characteristic time of the chemical reaction (t_{ch}) is much smaller than that of the fluid dynamical motion (t_{fl}), resulting in the Damköhler number (Da), defined as $Da = t_{fl}/t_{ch}$, being quite large. At $t = 180$ s, the region around the injection hole becomes clear, indicating that the more-viscous liquid has been completely displaced by the less-viscous liquid and that the less-viscous liquid completely sweeps the product. Fingers grow up, and the clear region becomes larger with further increase in t. These figures show that the viscous fingering patterns for the systems are similar with and without the chemical reaction, indicating that the chemical reaction can be treated as passive, as expected based on its heat release being negligible. This is different from active ones where the reaction significantly affects the fingering pattern by the production of a gradient in either viscosity (DeWit and Homsy, 1999a,b) or density (Carey et al., 1996; Vasquez, 1997; Eckert and Grahn, 1999).

Figure 4 shows the fingering patterns for systems with the chemical reaction for various sets of the initial molar concentrations of SCN^- (c_{m0}) and that of Fe^{3+} (c_{l0}) at $t = 390$ s. Figure 4a shows a case in which the ratio between c_{m0} and c_{l0} is stoichiometric, the same as in Figure 3, and the others show cases in which either c_{m0} or c_{l0} is increased or decreased from the condition depicted in Figure 4a. The viscous fingering patterns under all conditions are similar, once again indicating that the chemical reaction is passive under all experimental conditions. The depth of the blood-red color is deeper, that is, the quantity of the product increases in cases where either c_{m0} or c_{l0} is increased from the condition shown in Figure 4a (Figures 4b and 4d). These results indicate that the chemical reaction is diffusion-dominant; in other words, the reaction rate is much faster than the diffusion rate. This result corresponds to the observation in Figure 3 in that the chemical reaction starts immediately after injection. Otherwise, the amount of product would not increase even if the amount of either reactant were increased from the condition shown in Figure 4a. These results suggest that the stoichiometric ratio is a reference value in discussing the reaction pattern. We therefore introduce here a dimensionless parameter ϕ_v as follows

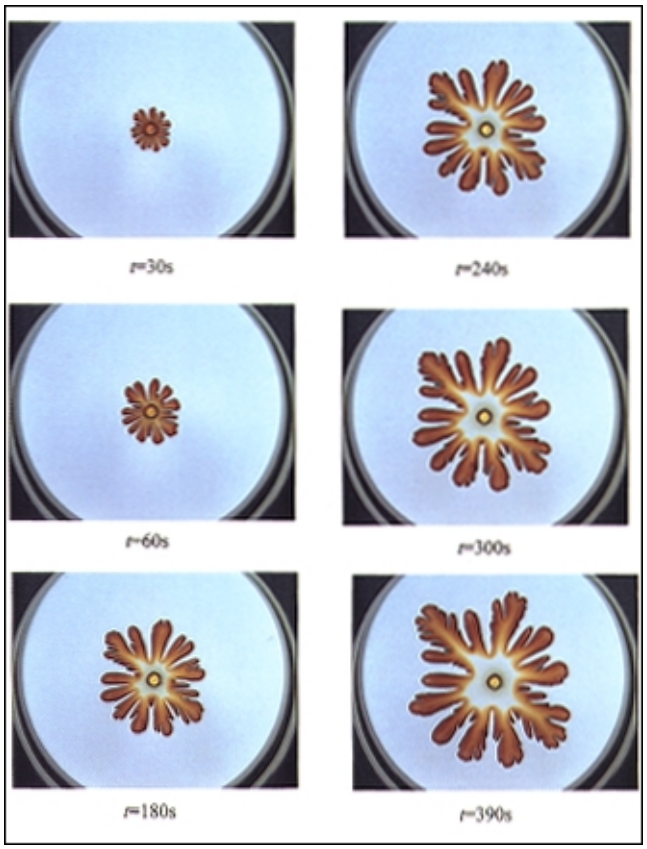

Figure 3. Temporal evolution of miscible viscous fingering with chemical reaction under conditions with $c_{m0} = 0.08$ mol/L and $c_{l0} = 0.04$ mol/L.

$$\phi_v = \frac{a c_{l0}}{c_{m0}} \tag{3}$$

Here, a denotes the molar stoichiometric ratio, and $a = 2$ in the present chemical reaction mentioned by Eq. 1. This parameter corresponds to the equivalence ratio widely used in combustion science (Warnatz et al., 1999). If the ratio between c_{m0} and c_{l0} is stoichiometric, $\phi_v = 1$. The location of the region where the product exists significantly depends particularly on ϕ_v. Figure 4a shows the reaction pattern in the case of $\phi_v = 1$. In this case, the depth of the blood-red color becomes gradually lighter toward the inside of the fingers. Figures 4c and 4d show the reaction patterns in the case where ϕ_v is sufficiently larger than 1. In this case, the color

depth at the fingertips is remarkably deep. On the other hand, when ϕ_v is sufficiently smaller than 1, the depth of the color is the deepest inside the fingers, as shown in Figures 4b and 4e. These results show that the product concentrates at the fingertips when c_{m0} is decreased or c_{l0} is increased ($\phi_v > 1$), while a certain amount of product spreads in a relatively broad area inside the fingers when c_{m0} is increased or c_{l0} is decreased ($\phi_v < 1$). In the present study, the finger growth velocity is low and the convection effects are weak, especially at the later stages of fingering due to the constant injection rate. Consequently, the location of the reaction zone is primarily determined by the molecular diffusion process of the reactants, and the product concentration reaches a maximum at the reaction zone. As a result, the variation in the region where the product exists significantly depends particularly on where the reaction zone is located. At $\phi_v = 1$, which is the stoichiometric condition, the reaction zone is located close to the interface between the less and more-viscous liquids, though it does not necessarily coincide completely with the interface. Since c_{m0} is increased or c_{l0} is decreased from the stoichiometric condition, that is, ϕ_v is sufficiently smaller than 1, the reaction zone is located far into the less-viscous liquid. Because $D \cdot \mu = \text{const.}$, the molecular diffusivity of the less-viscous liquid is larger than that of the more-viscous liquid by a factor of 1,200, which causes the product to spread widely in the less-viscous liquid, as ϕ_v is sufficiently smaller than 1. On the other hand, when ϕ_v is sufficiently larger than 1, the reaction zone is located very close to the interface in the more-viscous liquid, and the product scarcely diffuses in the more-viscous liquid. The product therefore concentrates close to the interface. The big difference in viscosity is one of the important factors in the formation of the viscous fingering, and it causes the large difference in molecular diffusivity, which results in the variations in the product distribution pattern. Thus, the variations in the product distribution pattern are a phenomenon inherent to reactive viscous fingering.

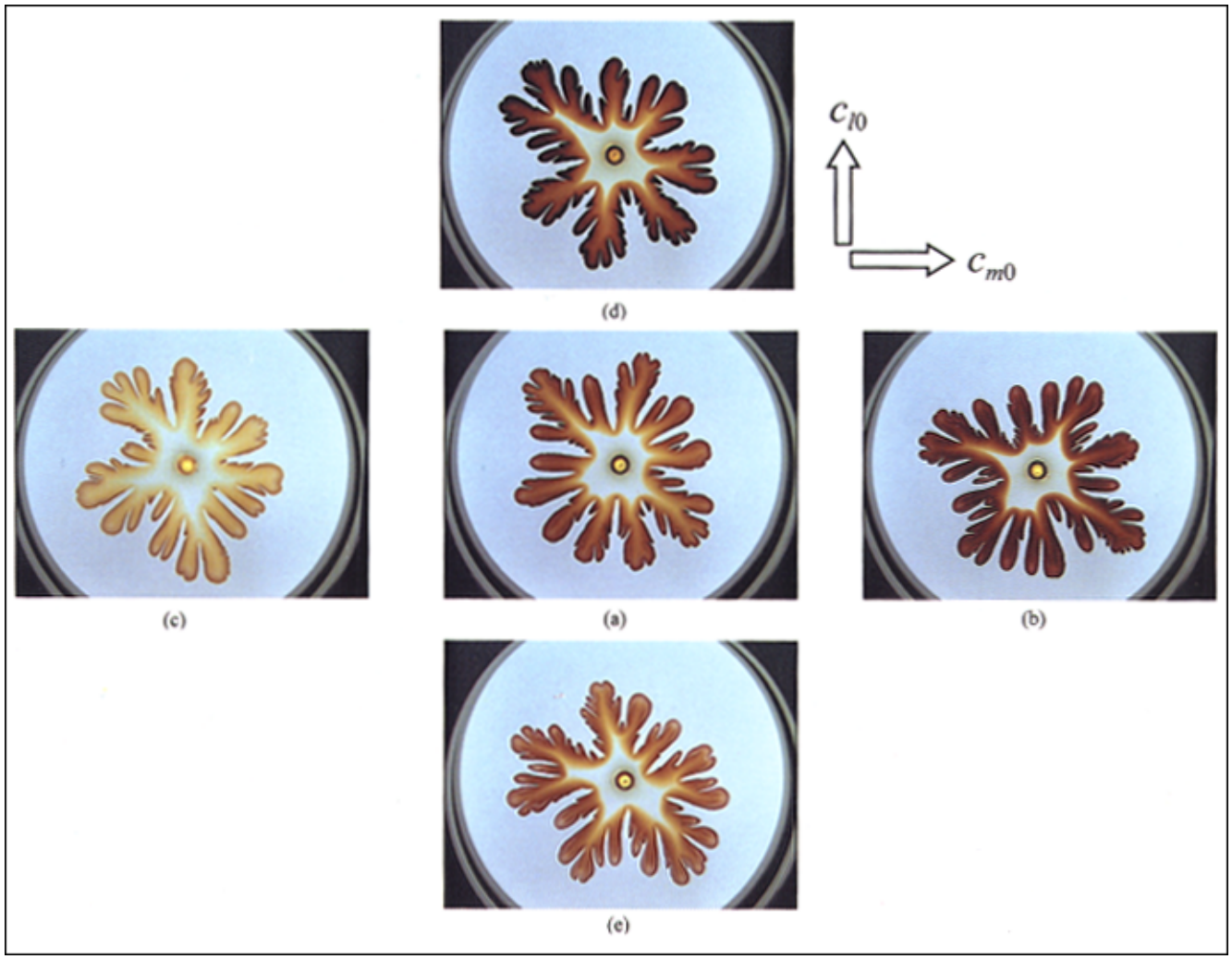

Figure 4. Fingering patterns with the chemical reaction for various sets of initial molar concentrations of SCN^- (c_{m0}) and that of Fe^{3+} (c_{l0}) at $t = 390$ s.

(a) $c_{m0} = 0.08$ mol/L, $c_{l0} = 0.04$ mol/L; (b) $c_{m0} = 0.3$ mol/L, $c_{l0} = 0.04$ mol/L; (c) $c_{m0} = 0.02$ mol/L, $c_{l0} = 0.04$ mol/L; (d) $c_{m0} = 0.08$ mol/L, $c_{l0} = 0.2$ mol/L; (e) $c_{m0} = 0.08$ mol/L, $c_{l0} = 0.02$ mol/L.

Analysis

Two types of product distribution patterns are shown in Figure 4. In one case, the product concentrates at the fingertips, while in the other case, the peak product concentration is located in the less-viscous liquid region. In this section, the variation in the product distribution pattern is discussed theoretically based on a simplified one-dimensional diffusion–reaction concept. The experimental results are modeled as described below:

1. A well-defined interface between two miscible liquids exists because $Pe_v \gg 1$ (Petitjeans and Maxworthy, 1996; Rakotomalala et al., 1997). Mass fluxes of reactants and product and the mass fractions of those are continuous at the interface.

2. The molecular diffusion coefficient of reactants and product are assumed to be D_m in the more-viscous liquid and D_l in the less-viscous liquid. The ratio between D_m and D_l, D_l/D_m is $D_l/D_m = \mu_m/\mu_l = 1.2\times10^3$, since the viscosity μ and diffusion coefficient D in liquids generally satisfy the following relationship, $D\cdot\mu = \text{const.}$.

3. The density of the less-viscous liquid, ρ_l, is estimated as $\rho_l = 1.00\times10^3$ kg/m^3, and that of the more-viscous liquid, ρ_m, is $\rho_m = 1.26\times10^3$ kg/m^3. Since the masses of reactants and product mixed in the liquids are less than 4.0%, their influence on the density is ignored.

4. In this study, the finger-growing velocity is low enough to neglect the convective transport of species, especially at the later stage of fingering due to the constant injection rate.

5. A steady state is assumed.

6. The molecular diffusion rate of reactants and product is given by Fick's law.

7. An instantaneous chemical reaction is assumed, as the chemical reaction takes place much faster than finger formation; in other words, the reaction is controlled by the molecular diffusion, as described earlier.

From these assumptions, the chemical species conservation equations become as follows

$$\rho D\frac{d^2Y_j}{dx^2} = 0. \tag{4}$$

Here x is the coordinate in the diffusion zone defined in detail in Figure 5. When the reactants and product diffuse in the less-viscous liquid, $\rho = \rho_l$ and $D = D_l$, and when they diffuse in the more-viscous liquid, $\rho = \rho_m$ and $D = D_m$. Also, Y_j is the mass fraction of j species, that is, two reactants and a product. Here, no reaction-rate term is included because the reaction rate in all regions except the infinitesimal reaction zone is zero. At the reaction zone, the reaction rate is infinite, and no reactants are assumed to exist there.

Figures 5a and 5b show the mass fraction model of two reactants and product in the case where the reaction surface is located in the less-viscous-liquid region and in the more-viscous-liquid region, respectively. Here Y_l is the mass fraction of the reactant, Fe^{3+}, Y_m is that of the reactant, SCN^-, and Y_p is that of the product, $[Fe(SCN)_2]^+$. The profiles of the reactants and product are linear, as predicted by Eq. 4, and the reaction zone is infinitesimal, as was already mentioned in the assumption 7. The abscissa is a dimensionless position x normalized by the width of the diffusion zone. The

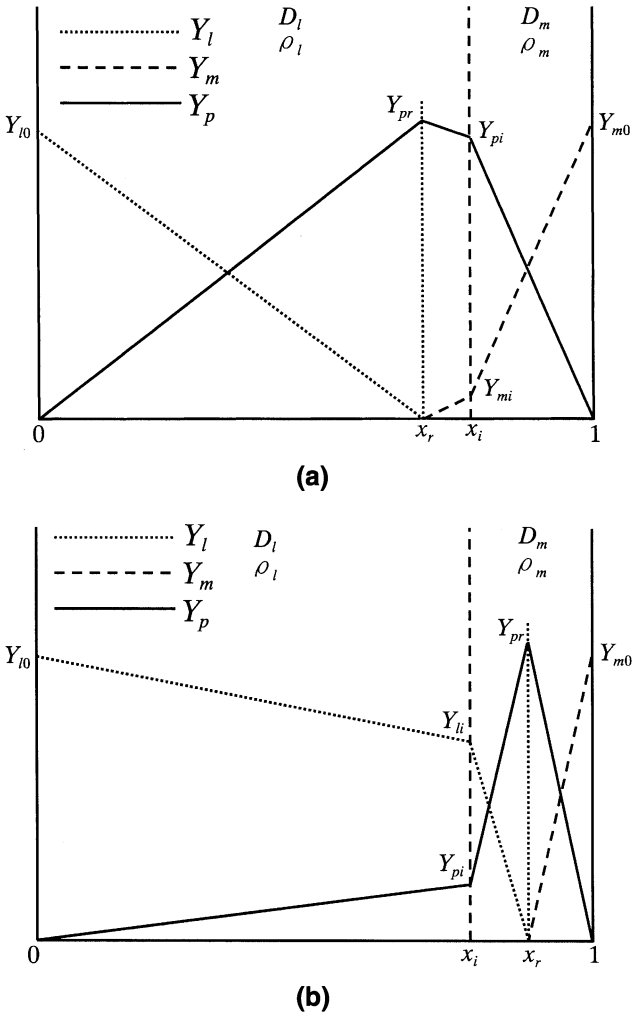

Figure 5. Mass fraction model of two reactants and product.

(a) reaction surface located in the less viscous liquid region ($x_r < x_i$); (b) reaction surface located in the more viscous liquid region ($x_i < x_r$).

less-viscous-liquid region is $0 \leqq x \leqq x_i$, and the more-viscous region is $x_i \leqq x \leqq 1$, where x_i is the position of the interface between two liquids.

In the case where the reaction surface is located in the less-viscous-liquid region (Figure 5a), the mass fluxes of the two reactants satisfy the following relations at the interface between the two liquids ($x = x_i$) according to the assumption 1, and at the reaction surface ($x = x_r$) according to the assumption 7

$$\rho_l D_l\frac{Y_{mi}}{x_i - x_r} = \rho_m D_m\frac{Y_{m0} - Y_{mi}}{1 - x_i} \quad (\text{at } x = x_i) \tag{5}$$

$$\alpha\rho_l D_l\frac{Y_{l0}}{x_r} = \rho_l D_l\frac{Y_{mi}}{x_i - x_r} \quad (\text{at } x = x_r). \tag{6}$$

Here, α denotes the mass stoichiometric ratio defined as Eq. 7.

$$\alpha = \frac{aM_m}{M_l} = \frac{29}{14} \tag{7}$$

Here, M_m is the molecular weight of SCN^-, $M_m = 58$, and M_l is the molecular weight of Fe^{3+}, $M_l = 56$, and $a = 2$, as mentioned before; Y_{m0} is the mass fraction of the reactant (SCN^-) at $x = 1$, Y_{mi} is that of SCN^- at $x = x_i$, and Y_{l0} is that of the reactant (Fe^{3+}) at $x = 0$. Because an instantaneous reaction (that is, an infinite reaction rate) is assumed, the location of the reaction surface x_r is algebraically related to the mass fraction of the two reactants at the boundaries ($x = 0$ and $x = 1$) and the location of the interface of the two liquids, x_i

$$x_r = \frac{\left\{\dfrac{D_l \rho_l}{D_m \rho_m}(1 - x_i) + x_i\right\}\dfrac{\alpha Y_{l0}}{Y_{m0}}}{1 + \dfrac{\alpha Y_{l0}}{Y_{m0}}} \quad (0 \leqq x_r \leqq x_i). \tag{8}$$

In the case where the reaction surface is located in the more-viscous-liquid region (Figure 5b), the analogous relations of Eqs. 5 and 6 are described as follows:

$$\rho_l D_l \frac{Y_{l0} - Y_{li}}{x_i} = \rho_m D_m \frac{Y_{li}}{x_r - x_i} \quad (\text{at } x = x_i) \tag{9}$$

$$\alpha \rho_m D_m \frac{Y_{li}}{x_r - x_i} = \rho_m D_m \frac{Y_{m0}}{1 - x_r} \quad (\text{at } x = x_r). \tag{10}$$

Here, Y_{li} is the mass fraction of the reactant (Fe^{3+}) at $x = x_i$. Therefore, x_r is obtained as follows:

$$x_r = \frac{\dfrac{\alpha Y_{l0}}{Y_{m0}} + x_i\left(1 - \dfrac{D_m \rho_m}{D_l \rho_l}\right)}{1 + \dfrac{\alpha Y_{l0}}{Y_{m0}}} \quad (x_i \leqq x_r \leqq 1). \tag{11}$$

It is appropriate that the widths of the diffusion zones in the more- and less-viscous liquids are proportional to the value of ρD, and then x_i satisfies the following relation:

$$x_i : 1 - x_i = \rho_l D_l : \rho_m D_m. \tag{12}$$

Because $\rho_l D_l : \rho_m D_m \approx 1200 : 1.26$, the value of x_i is solved as about 0.999, meaning that the interface between the two liquids is located quite close to the more-viscous-liquid boundary ($x = 1$).

At the reaction surface, mass fractions of the reactants and the product satisfy Eq. 13 in the case of $0 \leqq x_r \leqq x_i$, and Eq. 14 in the case of $x_i \leqq x_r \leqq 1$, because of mass conservation, indicating the sum of the fluxes of the reactants into the reaction surface is equal to the flux of the product out from the reaction surface:

$$\rho_l D_l \frac{Y_{l0}}{x_r} + \rho_l D_l \frac{Y_{mi}}{x_i - x_r} = \rho_l D_l \frac{Y_{pr}}{x_r} + \rho_l D_l \frac{Y_{pr} - Y_{pi}}{x_i - x_r} \quad (\text{at } x = x_r)\ (0 \leqq x_r \leqq x_i) \tag{13}$$

$$\rho_m D_m \frac{Y_{li}}{x_r - x_i} + \rho_m D_m \frac{Y_{m0}}{1 - x_r} = \rho_m D_m \frac{Y_{pr} - Y_{pi}}{x_r - x_i} + \rho_m D_m \frac{Y_{pr}}{1 - x_r} \quad (\text{at } x = x_r)\ (x_i \leqq x_r \leqq 1) \tag{14}$$

where Y_{pr} is the mass fraction of the product ($[Fe(SCN)_2]^+$) at $x = x_r$ and Y_{pi} is that at $x = x_i$. Furthermore, Y_{pr} and Y_{pi} satisfy Eq. 15 in the case of $0 \leqq x_r \leqq x_i$ and Eq. 16 in the case of $x_i \leqq x_r \leqq 1$ at the interface because of the assumption 1.

$$\rho_l D_l \frac{Y_{pr} - Y_{pi}}{x_i - x_r} = \rho_m D_m \frac{Y_{pi}}{1 - x_i} \quad (\text{at } x = x_i)\ (0 \leqq x_r \leqq x_i) \tag{15}$$

$$\rho_l D_l \frac{Y_{pi}}{x_i} = \rho_m D_m \frac{Y_{pr} - Y_{pi}}{x_r - x_i} \quad (\text{at } x = x_i)\ (x_i \leqq x_r \leqq 1). \tag{16}$$

By using Eqs. 6, 13, and 15 in the case of $0 \leqq x_r \leqq x_i$, or Eqs. 10, 14, and 16 in the case of $x_i \leqq x_r \leqq 1$, Y_{pr} is determined as Eq. 17.

$$Y_{pr} = \frac{(\alpha + 1) Y_{l0} Y_{m0}}{\alpha Y_{l0} + Y_{m0}}. \tag{17}$$

The effect of the initial molar concentrations of reactant on the location of the reaction surface, x_r, and the molar concentration of the product at x_r, c_{pr}, is shown in Figure 6. Here the values of reactants and product are shown as molar concentrations in order to compare these results with the experimental results. The molar concentrations of reactants are obtained by Eq. 18 and Eq. 19. The molar concentrations of product are obtained by Eq. 20 as $0 \leqq x_r \leqq x_i$, or by Eq. 21 as $x_i \leqq x_r \leqq 1$. Here, M_p is the molecular weight of the product, $[Fe(SCN)_2]^+$, $M_p = 172$

$$c_{l0} = \frac{\rho_l Y_{l0}}{M_l} \tag{18}$$

$$c_{m0} = \frac{\rho_m Y_{m0}}{M_m} \tag{19}$$

$$c_{pr} = \frac{\rho_l Y_{pr}}{M_p} \tag{20}$$

$$c_{pr} = \frac{\rho_m Y_{pr}}{M_p}. \tag{21}$$

Variations in x_r and c_{pr} with c_{l0} under the condition of constant $c_{m0} = 0.08$ mol/L are shown in Figure 6a. The left ordinate has two different scales at $0 \leqq x \leqq 0.95$ and at $0.998 \leqq x \leqq 1$ in order to make it easy to identify the variations in x_r with c_{l0}. As shown in Figure 6a, under the condition of con-

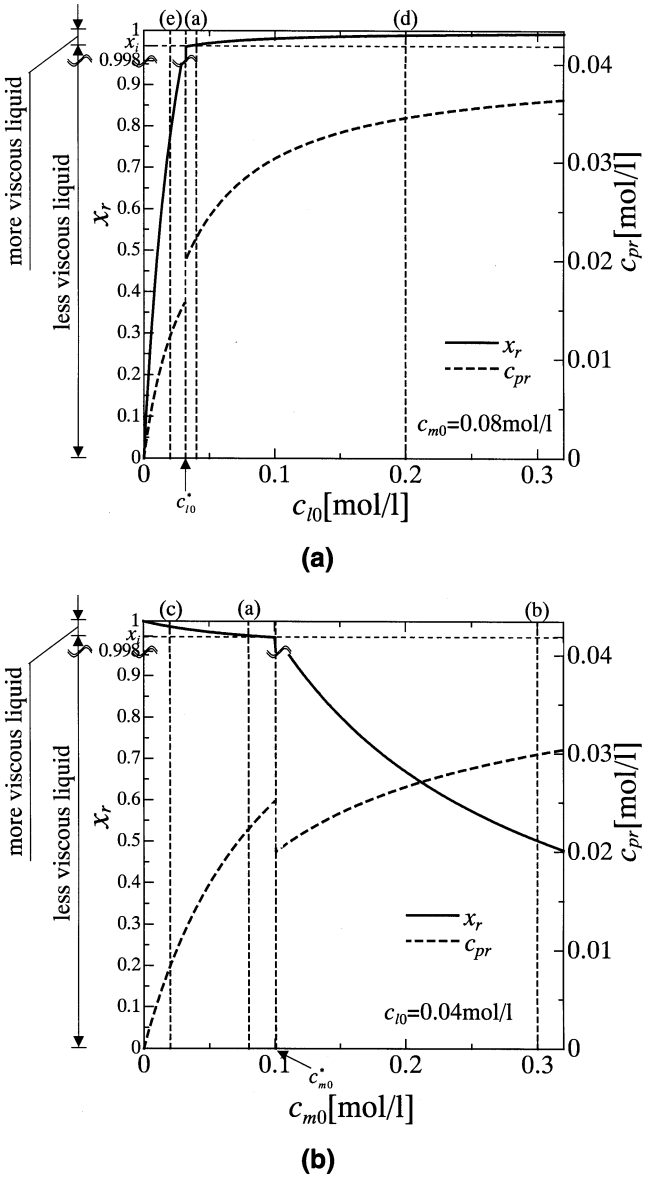

Figure 6. Effect of initial molar concentration of reactants on the location of the reaction surface, x_r, and the molar concentration of the product at x_r, c_{pr}.

(a): Variations in x_r and c_{pr} with c_{l0} under the condition that $c_{m0} = 0.08$ mol/L; (b) Variations in x_r and c_{pr} with c_{m0} under the condition that $c_{l0} = 0.04$ mol/L.

stant $c_{m0} = 0.08$ mol/L, x_r becomes equal to x_i as $c_{l0} = c^*_{l0} = 0.0317$ mol/L. As $c_{l0} > c^*_{l0}$, x_r is located in the more-viscous-liquid region, and x_r then varies only between $x = 0.999$ and $x = 1$ even when c_{l0} is varied because of $x_i = 0.999$. As a result, x_r scarcely varies as $c_{l0} > c^*_{l0}$. In contrast, as $c_{l0} < c^*_{l0}$, x_r is located in the less-viscous-liquid region, and x_r varies widely in the less-viscous liquid when c_{l0} is varied. The condition of Figure 4a is shown as (a) in Figure 6a. In this case, x_r almost overlaps with x_i. The condition of Figure 4d is shown as (d) in Figure 6a. In this case, x_r is located in the more viscous liquid. The condition of Figure 4e is shown as

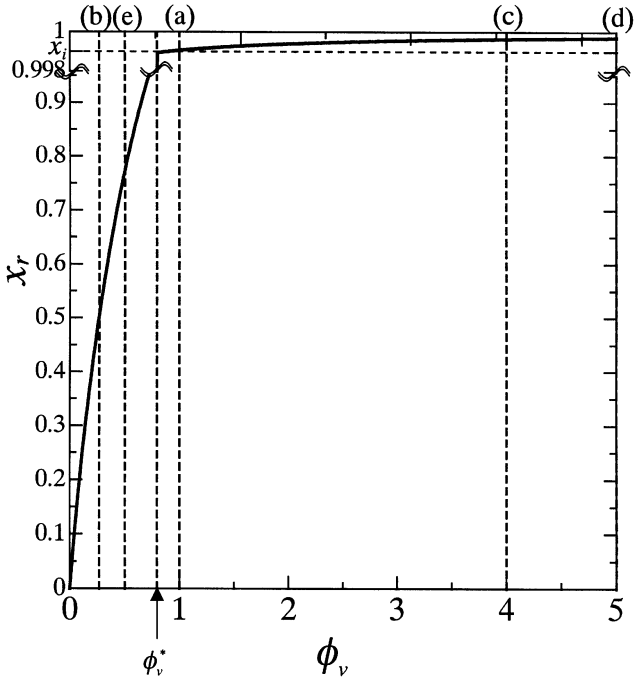

Figure 7. Variations in x_r with ϕ_v.

(e) in Figure 6a. In this case, x_r is located in the less-viscous liquid. The molar concentration of the product at x_r, c_{pr} increases with an increase in c_{l0}. In the present study, Y_{pr} is continuous in all regions as shown in Eq. 17. Thus, the profile of c_{pr} becomes discontinuous at $c_{l0} = c^*_{l0}$ because c_{pr} can be calculated by Eqs. 20 and 21 as $x_r = x_i$, as mentioned before; c_{pr} increases from (e) to (a) to (d), as shown in Figure 6a. These results qualitatively agree with the experimental results shown in Figure 4. Variations in x_r and c_{pr} with c_{m0} under the condition of constant $c_{l0} = 0.04$ mol/L are shown in Figure 6b. The left ordinate also has two different scales at $0 \leqq x \leqq 0.95$ and $0.998 \leqq x \leqq 1$ in order to make it easy to identify the variations in x_r with c_{m0}; x_r becomes equal to x_i as $c_{m0} = c^*_{m0} = 0.101$ mol/L. As $c_{m0} < c^*_{m0}$, x_r is located in the more-viscous-liquid region and as a result, x_r scarcely varies with the variations in c_{m0}. In contrast, as $c_{m0} > c^*_{m0}$, x_r is located in the less-viscous-liquid region, and x_r varies widely in the less-viscous liquid with variations in c_{m0}. The profile of c_{pr} increases with c_{m0}, except $c_{m0} = c^*_{m0}$. At $c_{m0} = c^*_{m0}$, as well as in Figure 6a, the profile of c_{pr} is not continuous. The conditions in Figures 4a, 4b, and 4c are shown as (a), (b), and (c) in Figure 6b. Here, c_{pr} increases from (c) to (a) to (b), which corresponds to Figures 4c, 4a, and 4b.

By using ϕ_v, the effect of reactant concentrations at the boundaries ($x = 0$ and $x = 1$) on the location of x_r can be discussed much more clearly, as shown in Figure 7. In the figure, ϕ^*_v, which is the value of ϕ_v as $x_r = x_i$, is obtained by Eq. 22 from Eqs. 8 and 12, or Eqs. 11 and 12

$$\phi^*_v = \frac{\rho_l}{\rho_m} \approx 0.794 \tag{22}$$

When $\phi_v > \phi^*_v$, x_r is located in the more-viscous-liquid region, and x_r scarcely varies with the variation in ϕ_v. How-

ever, when $\phi_v < \phi_v^*$, x_r is located in the less-viscous-liquid region, and x_r varies widely in the less-viscous liquid with the variation in ϕ_v. In summary, when x_r is located in the more-viscous-liquid region, x_r scarcely varies with the variation in ϕ_v, while when x_r is located in the less-viscous-liquid region, x_r varies widely in the less-viscous-liquid region with the variations in ϕ_v. This difference in mobility of x_r in the two liquids is due to the large difference in the molecular diffusion coefficients.

The profiles of molar concentration of the reactants Fe^{3+} (c_l) and SCN^- (c_m) and that of the product $[Fe(SCN)_2]^+$ (c_p) under the conditions in Figures 4a–4e are shown in Figures 8a–8e. Here, in order to compare the theoretical results with the experimental ones, the mass fractions of j species Y_j are transformed into the molar concentrations of j species c_j by Eq. 23 in the less-viscous liquid and by Eq. 24 in the more-viscous liquid. Here, M_j are the molecular weights of j species

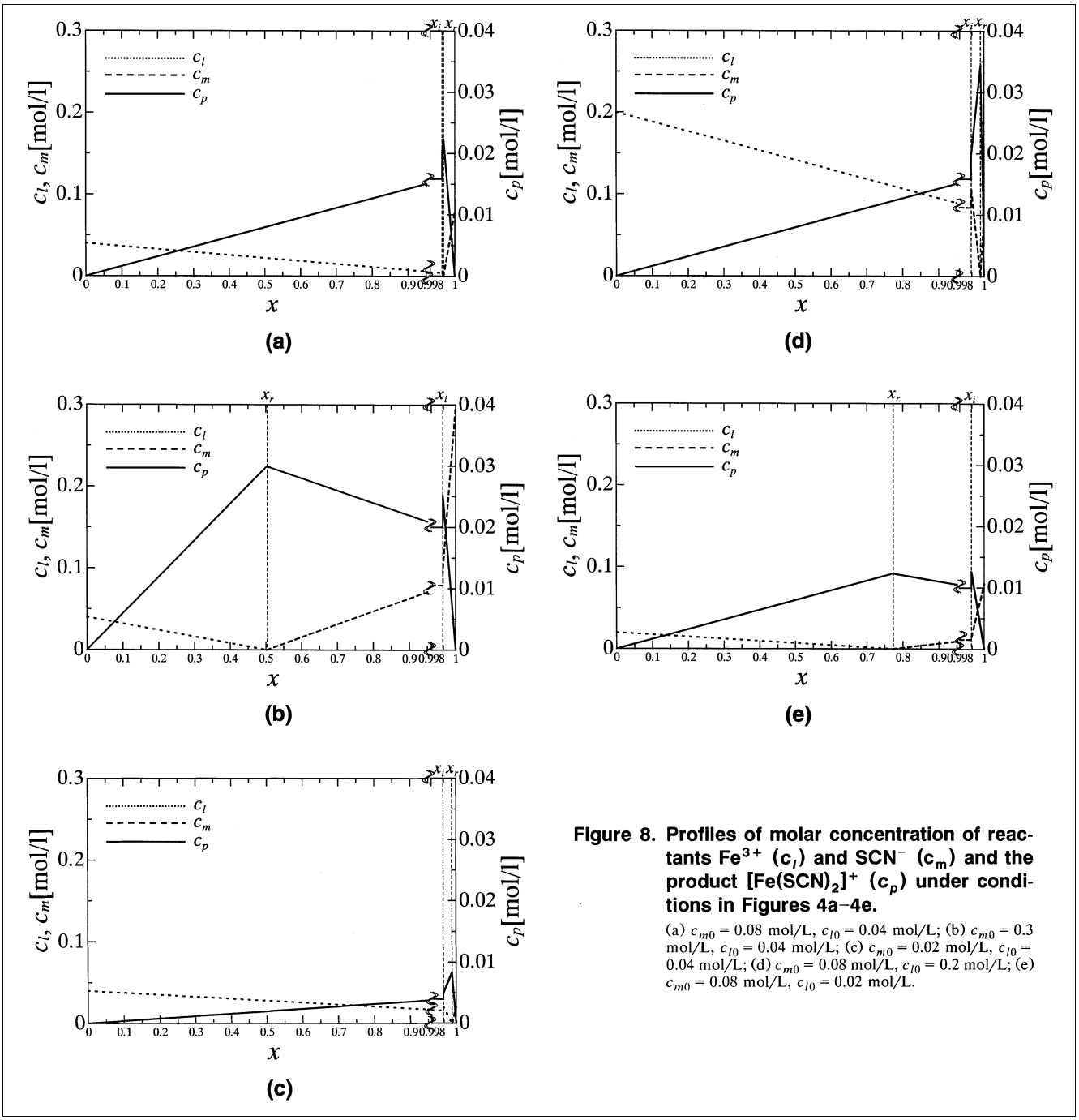

Figure 8. Profiles of molar concentration of reactants Fe^{3+} (c_l) and SCN^- (c_m) and the product $[Fe(SCN)_2]^+$ (c_p) under conditions in Figures 4a–4e.

(a) c_{m0} = 0.08 mol/L, c_{l0} = 0.04 mol/L; (b) c_{m0} = 0.3 mol/L, c_{l0} = 0.04 mol/L; (c) c_{m0} = 0.02 mol/L, c_{l0} = 0.04 mol/L; (d) c_{m0} = 0.08 mol/L, c_{l0} = 0.2 mol/L; (e) c_{m0} = 0.08 mol/L, c_{l0} = 0.02 mol/L.

$$c_j = \frac{\rho_l Y_j}{M_j} \tag{23}$$

$$c_j = \frac{\rho_m Y_j}{M_j}. \tag{24}$$

In order to make it easy to identify the profiles of the molar concentrations of the reactants and product, the abscissa has two different scales at $0 \leqq x \leqq 0.95$ and at $0.998 \leqq x \leqq 1$. The molar concentrations of those at x_i are not continuous, since their mass fractions are continuous. The jump in molar concentration at x_i is due to $\rho_m > \rho_l$. At $\phi_v = 1$, x_r is almost equal to x_i, and the molar concentration of the product (c_p) decreases gradually toward the side of the less-viscous liquid (Figure 8a). In the case where ϕ_v is sufficiently larger than 1, x_r moves to the side of the more-viscous liquid from the case of $\phi_v = 1$, and c_p drops approximately half from x_r to x_i in the more-viscous-liquid region, indicating that the product is concentrated around x_i (Figures 8c, 8d). In the case where ϕ_v is sufficiently smaller than 1, x_r moves far into the less-viscous liquid, and a certain amount of product exists in a relatively broad area in the less-viscous liquid. (Figures 8b, 8e). As mentioned earlier, the experimental and theoretical results are in good agreement, confirming that the significant differences in the product distribution within fingers are due to shifts in the reaction zone between less- and more-viscous liquid.

As described for the nonreactive case, the fingertips have a three-dimensional structure that can be drawn as shown in Figure 9 (Lajeunesse et al., 1999). When the reaction surface is located in the more-viscous-liquid region, the results of the present study suggest that the reaction surface is formed along the interface between the two liquids, as shown in Figure 9a, and the product scarcely diffuses in the more-viscous liquid,

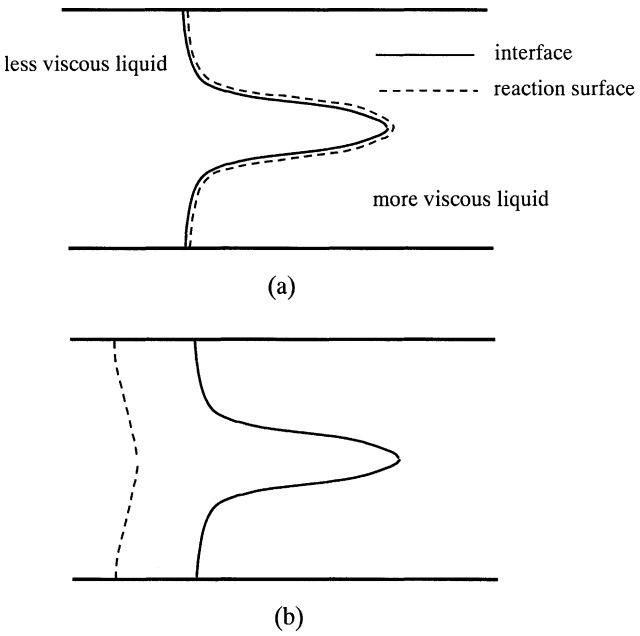

Figure 9. Three-dimensional structure at fingertips.

(a) reaction surface located in the more viscous liquid region; (b) reaction surface located in the less viscous liquid region.

concentrating along the interface in the fingertips. In fact, the region where experimentally observed product concentrates corresponds to fingertips in the nonreactive case where the depth of the blood-red color is light, as shown in Figure 2. As a result, this region is broader than that predicted theoretically. In contrast, when the reaction surface moves to the less-viscous side, as shown in Figure 9b, the reaction surface leaves the interface, becoming almost two-dimensional. These results suggest that the three-dimensional structure at the fingertips does not influence the present result except in the region where the product concentrates is slightly broader at the fingertips.

In summary, the present study has shown that differences in molecular diffusivity, that is, viscosity, play a key role in determining the reaction pattern. Because a difference in viscosity between two liquids is necessary for viscous fingering, variations in the reaction pattern are inherent characteristics of reactive viscous fingering.

Conclusion

The effects of reactant concentrations on the characteristics of reactive miscible viscous fingering with low finger-growth velocity were investigated using a Hele-Shaw cell. When the less-viscous liquid, a $Fe(NO)_3$ solution, displaced the more-viscous one, a mixture of 99 wt % glycerin and 1 wt % KSCN solution, in the cell, a fingering pattern was formed with the following chemical reaction: Fe^{3+}(light yellow) + $2SCN^-$(colorless) $\rightarrow [Fe(SCN)_2]^+$(blood red). Experiments were carried out by varying the initial molar concentrations of reactants in both liquids, and a nonreactive experiment was performed to compare with the reactive ones. When the initial reactant concentration in either the more-viscous liquid, c_{m0}, or the less-viscous liquid, c_{l0}, is increased from the stoichiometric condition, more product is formed, indicating that the chemical reaction is diffusion-controlled. The distribution of product varies with the variations in the initial reactant concentrations, and depends on where a reaction zone is located. When the reaction zone is located in the more-viscous-liquid region, the product concentrates at the fingertips, while when it is located in the less-viscous-liquid region, the product spreads in a relatively broad area inside the fingers. This shift in reaction zones resulting from variations in the reactant concentrations produced significant difference in the distribution of product. A dimensionless parameter $\phi_v = 2c_{l0}/c_{m0}$ is proposed. When ϕ_v is sufficiently large compared to 1, the reaction zone is located in the more-viscous-liquid region, and the product concentrates at the finger tips. In contrast, when ϕ_v is sufficiently small compared to 1, the reaction zone is located in the less-viscous-liquid region, and the product spreads in a relatively broad area inside the fingers. These results suggest that the differences in molecular diffusivity, that is, viscosity, play a key role in determining the reaction pattern. Because a difference in viscosity between two liquids is necessary for viscous fingering, variations in the reaction pattern are inherent characteristics of reactive viscous fingering.

Literature Cited

Bhaskar, K. R., P. Garik, B. S. Turner, J. D. Bradley, R. Bansil, H. E. Stanley, and J. T. LaMont, "Viscous Fingering of HCl Through Gastric Mucin," *Nature*, **360**, 458 (1992).

Carey, M. R., S. W. Morris, and P. Kolodner, "Convective Fingering of Autocatalytic Reaction Front," *Phys. Rev. E*, **53**, 6012 (1996).
Chen, J.-D. "Growth of Radial Viscous Fingers in a Hele-Shaw Cell.," *J. Fluid Mech.*, **201**, 223 (1989).
Chu, S., S. Tanaka, J. D. Kaunitz, and M. H. Montrose, "Dynamic Regulation of Gastric Surface pH by Luminal pH," *J. Clin. Invest.*, **103**, 605 (1999).
DeWit, A., and G. M. Homsy, "Viscous Fingering in Reaction-Diffusion Systems," *J. Chem. Phys.*, **110**(17) 8663 (1999a).
DeWit, A., and G. M. Homsy, "Nonlinear Interaction of Chemical Reactions and Viscous Fingering in Porous Media," *Phys. Fluids*, **11**, 949 (1999b).
Dickson, M. L., T. T. Norton, and E. J. Fernandez, "Chemical Imaging of Multicomponent Viscous Fingering in Chromatography," *AIChE J.*, **43**, 409 (1997).
Eckert, K., and A. Grahn, "Plume and Finger Regimes Driven by an Exothermic Interfacial Reaction," *Phys. Rev. Lett.*, **82**, 4436 (1999).
Homsy, G. M., "Viscous Fingering in Porous Media," *Annu. Rev. Fluid Mech.*, **19**, 271 (1987)
Hornof, V., and F. U. Baig, "Influence of Interfacial Reaction and Mobility Ratio on the Displacement in a Hele-Shaw Cell," *Exp. Fluids*, **18**, 448 (1995).
Lajeunesse, E., J. Martin, N. Rakotomalala, D. Salin, and Y. C. Yortsos, "Miscible Displacement in a Hele-Shaw Cell at High Rates," *J. Fluid Mech.*, **398**, 299 (1999).
Petitjeans, P., C. Y. Chen, E. Meiburg, and T. Maxworthy, "Miscible Quarter Five-Spot Displacements in a Hele-Shaw Cell and the Role of Flow-Induced Dispersion," *Phys. Fluids*, **11**, 1705 (1999).
Petitjeans, P., and T. Maxworthy, "Miscible Displacement in Capillary Tubes. Part 1. Experiment," *J. Fluid Mech.*, **326**, 37 (1996).
Pojman, J. A., G. Gunn, C. Patterson, J. Owens, and C. Simmons, "Frontal Dispersion Polymerization," *J. Phys. Chem.*, **102**, 3927 (1998).
Rakotomalala, N., D. Salin, and P. Watzky, "Miscible Displacement Between Two Parallel Plates: BGK Lattice Gas Simulations," *J. Fluid Mech.*, **338**, 277 (1997).
Shalliker, R. A., B. S. Broyles, and G. Guiochon, "Visualization of Viscous Fingering in High-Performance Liquid Chromatographic Columns-Influence of the Header Design," *J. Chromatog. A*, **865**, 73 (1999).
Tanveer, S., "Surprises in Viscous Fingering," *J. Fluid Mech.*, **409**, 273 (2000).
Vasquez, D. A., "Linear Stability Analysis of Convective Chemical Fronts," *Phys. Rev. E*, **56** 6767 (1997).
Warnatz, J., U. Maas, and R. W. Dibble, *Combustion*, 2nd ed., Springer-Verlag, Berlin (1999).
Zidansek, A., A. Blinc, G. Lahajnar, D. Keber, and R. Blinc, "Finger-Like Lysing Patterns of Blood Clots," *Biophys. J.*, **69**, 803 (1995).

Manuscript received Aug. 8, 2000, and revision received Mar. 20, 2001.